

TECHNICAL MEMORANDUMS
NATIONAL ADVISORY COMMITTEE FOR AERONAUTICS

No 336

PRESSURE DISTRIBUTION ON JOUKOWSKI WINGS

By Otto Blumenthal

and

GRAPHIC CONSTRUCTION OF JOUKOWSKI WINGS

By E. Trefftz

From "Zeitschrift für Flugtechnik und Motorluftschiffahrt,"
May 31, 1913

Washington
October, 1925

NATIONAL ADVISORY COMMITTEE FOR AERONAUTICS.

TECHNICAL MEMORANDUM NO. 336.

PRESSURE DISTRIBUTION ON JOUKOWSKI WINGS.*

By Otto Blumenthal.

In the winter semester of 1911-12, I described, in a lecture on the hydrodynamic bases of the problem of flight, the potential flow about a Joukowski wing.** In connection with this lecture, Karl Toepfer and Erich Trefftz computed the pressure distribution on several typical wings and plotted their results. I now publish these diagrams accompanied by a qualitative discussion of the pressure distribution, which sufficiently indicates the various possible phenomena. For a quicker survey, I have divided the article into two parts, the first part dealing with the more mathematical and hydrodynamic aspects and the second part, which is comprehensible in itself, taking up the real discussion from the practical standpoint.

* From "Zeitschrift für Flugtechnik und Motorluftschiffahrt,"
May 31, 1913.

** See above magazine, Vol. I (1910), p. 281.

I

We obtain the entire number of all Joukowski wings of the length $2l$ with the trailing edge at the point $x = -l$, by laying, in a $\zeta = \xi + i\eta$ plane through the point $\zeta = l/2$, the cluster of all the circles which contain the point $\zeta = l/2$, either inside or on their circumference, and plotting these circles by means of the formula

$$z = \zeta + \frac{l^2}{4\zeta} \quad (1)$$

on the $z = x + iy$ plane. The circles, which contain the point $\zeta = l/2$ on their circumference, thus become doubly intersected arcs and, in particular, the circle, which has the distance $(-l/2, +l/2)$ for its diameter, becomes the rectilinear distance of the length $2l$. The circles which contain the point $\zeta = l/2$ inside, furnish the real Joukowski figures. The point $\zeta = -l/2$ passes every time into the sharp trailing edge. The individual Joukowski wings are characterized by the following quantities (Fig. 1). The center M of the circle K is connected with the point H , $\zeta = -l/2$, and the point of intersection of this connecting line with the η axis is designated by M' . The distance OM' on the η axis is equal to half the height of the arc produced by describing the circle about M' as its center and is therefore designated by $f/2$, as half the camber of the Joukowski wing, f being its first characteristic dimension. We have chosen as the

second characteristic dimension, the radii difference $MM' = \delta$. This gives a measurement for the thickness of the Joukowski wing.

We will now consider the determination of the velocity and pressure distribution which produce an air flow along the wing, in infinity, with the velocity V at an angle of $\pi - \beta$ with the positive x axis, β being the angle of attack of the wing.

The absolute velocity q of this flow is calculated thus: If $\kappa(\xi, \eta)$ is the absolute velocity of the air flow, of velocity V and angle of attack β , around the circle K in the ζ plane, then

$$q(x, y) = \frac{\kappa(\xi, \eta)}{\left| \frac{dz}{d\xi} \right|}$$

It is, however,

$$\left| \frac{dz}{d\xi} \right| = \frac{1}{\sigma^2} \sqrt{(\sigma^2 - \frac{l^2}{4})^2 + l^2 \eta^2}, \quad \sigma^2 = \xi^2 + \eta^2,$$

and along the circle K

$$\kappa(\xi, \eta) = \frac{1}{\frac{\sqrt{l^2 + \xi^2}}{2} + \delta} \left| 2V(\xi \sin\beta + \eta \cos\beta) + c \right|,$$

where $2\pi c$ is the circulation. This constant is determined according to Kutta, by the condition that the velocity at the trailing edge is finite and therefore, since $dz/d\xi$ there disappears, κ must also disappear at the point H . Thus we obtain

$$\left. \begin{aligned} \kappa(\xi, \eta) &= \frac{1}{\frac{\sqrt{l^2 + f^2}}{2} + \delta} \cdot 2 \left| \left(\xi + \frac{l}{2} \right) \sin\beta + \eta \cos\beta \right|, \\ \frac{q}{V} &= \frac{\sigma^2}{\frac{\sqrt{l^2 + f^2}}{2} + \delta} \cdot \frac{2 \left| \left(\xi + \frac{l}{2} \right) \sin\beta + \eta \cos\beta \right|}{\sqrt{\left(\sigma^2 - \frac{l^2}{4} \right)^2 + l^2 \eta^2}} \end{aligned} \right\} (2)$$

$$\sigma^2 = \xi^2 + \eta^2.$$

This rather involved expression is simplified by the introduction of a new variable, the angle ω at the center of the circle K , measured from the radius MH . In this angle, the coordinates ξ, η and the quantities connected with them are expressed as follows: For abbreviation, we designate the radius of the circle K with $r = \frac{\sqrt{l^2 + f^2}}{2} + \delta$ and introduce the angle A by

$$\cos A = \frac{l}{\sqrt{l^2 + f^2}}, \quad \sin A = \frac{f}{\sqrt{l^2 + f^2}}.$$

The geometric significance of A and ω is obvious from Fig. 1.

By simple calculations we now obtain

$$\left. \begin{aligned} \xi &= -\frac{l}{2} + 2r \sin \frac{\omega}{2} \sin \left(\frac{\omega}{2} + A \right), \\ \eta &= -2r \sin \frac{\omega}{2} \cos \left(\frac{\omega}{2} + A \right), \end{aligned} \right\} (3)$$

$$\left. \begin{aligned} \sigma^2 &= \frac{l^2}{4} - 2l r \sin \frac{\omega}{2} \cdot \sin \left(\frac{\omega}{2} + A \right) + 4 r^2 \sin^2 \frac{\omega}{2} \\ &= \frac{l^2}{4} + 4 r \sin \frac{\omega}{2} \left[\delta \sin \frac{\omega}{2} - \frac{f}{2} \cos \left(\frac{\omega}{2} + A \right) \right] \end{aligned} \right\} (4)$$

Formula 2 for q is simplified by the introduction of the angle ω , to

$$\left. \begin{aligned} \left| \frac{q}{V} \right| &= \frac{\sigma^2}{r \frac{l}{2}} \\ \dots \dots \dots \left| \cos \left(\frac{\omega}{2} + A + \beta \right) \right| \dots \dots \dots \\ \sqrt{\cos^2 \left(\frac{\omega}{2} + A \right) + \frac{4}{l^2} \left[\delta \sin \frac{\omega}{2} - \frac{f}{2} \cos \left(\frac{\omega}{2} + A \right) \right]^2} \\ &= \frac{\sigma^2}{r \frac{l}{2}} F \end{aligned} \right\} (5)$$

From this we next derive a few general results which hold good for all the quantities f, δ, β .

a) On the trailing edge $\frac{q}{V} = \frac{l}{2r} \cos(A + \beta)$.

b) On top of the wing, there is always a portion along which the velocity $q > V$, hence where there is a negative pressure. As proof of this, we will consider the center of the upper side, the point $\omega = \frac{3\pi}{2} - A$. At this point $\sigma > r$, as can easily be seen geometrically (Fig. 1) or from formula 4. However, if we put $\omega = \frac{3\pi}{2} - A$ in formula 5, it then becomes

$$\left| \frac{q}{V} \right| = \frac{\sigma^2}{r \frac{l}{2}} \frac{\cos \left(\frac{\pi}{4} - \frac{A}{2} - \beta \right)}{\cos \left(\frac{\pi}{4} - \frac{A}{2} \right)} \frac{1}{\sqrt{1 + \frac{4}{l^2} \left(\delta + \frac{f}{2} \right)^2}}$$

$$> \frac{\cos \left(\frac{\pi}{4} - \frac{A}{2} - \beta \right)}{\cos \left(\frac{\pi}{4} - \frac{A}{2} \right)} \frac{r}{\sqrt{\frac{l^2}{4} + \left(\delta + \frac{f}{2} \right)^2}} > \frac{\cos \left(\frac{\pi}{4} - \frac{A}{2} - \beta \right)}{\cos \left(\frac{\pi}{4} - \frac{A}{2} \right)}$$

c) The velocity is zero at the point $\omega = \pi - 2A - 2\beta$, which is always located on the lower side. At this point the streamline enters the wing. Further general conclusions (i.e., applying to all f, δ, β) can hardly be drawn. We obtain considerably more accurate expressions in the especially interesting practical case where, in the vicinity of the leading edge, a pronounced velocity maximum and consequently a strong suction is produced. We will confine ourselves to this case in all that follows. Hereby we can, in formula 5, first of all disregard the slight fluctuation of the factor σ^2 for small values of f and δ and consider only the factor F , which must be alone decisive for the great changes in velocity. This factor, however, enables a simple explanation.

For this purpose, we introduce the angle $\psi = \frac{\omega}{2} + A + \beta$. The entering point of the streamline then lies at $\psi = \pi/2$, where F disappears. In general, we have

$$\frac{1}{F^2} = (a^2 + \sin^2\beta) \tan^2 \psi - 2 (ab - \sin\beta \cos\beta) \tan\psi + (b^2 + \cos^2\beta),$$

$$\left. \begin{aligned} a &= \frac{2}{l} \left(\delta \cos (A + \beta) - \frac{f}{2} \sin\beta \right), \\ b &= \frac{2}{l} \left(\delta \sin (A + \beta) + \frac{f}{2} \cos\beta \right). \end{aligned} \right\} \quad (6)$$

Consequently, F attains its maximum value at the angle ψ_0 , which is given by the formula

$$\tan \psi_0 = \frac{ab - \sin\beta \cos\beta}{a^2 + \sin^2\beta} \quad (7)$$

and this value is

$$F_{\max} = \frac{\sqrt{\left(\delta \cos (A + \beta) - \frac{f}{2} \sin \beta\right)^2 + \frac{l^2}{4} \sin^2 \beta}}{\delta \cos A} \quad (7')$$

We now make the assumption, corresponding to the already announced purpose of our investigation, that F has a high maximum in relation to the value of $\cos (A + \beta)$ on the trailing edge. We require, e.g., that F_{\max} shall equal or exceed $\sqrt{2}$. This is mathematically the most favorable. Formula 7', with the aid of a rough estimate, then gives

$$\begin{aligned} \frac{\sqrt{l^2 + f^2}}{2} \sin \beta &\geq \delta \cos (A + \beta) \left(1 + \frac{f}{\sqrt{l^2 + f^2}}\right) \\ &= \delta \cos (A + \beta) (1 + \sin A) \dots \quad (8) \end{aligned}$$

With this insertion, the numerator of $\tan \psi_0$ is smaller than

$$-\frac{4\delta}{l} \cos (A + \beta) \left[\frac{\sqrt{l^2 + f^2}}{2} \cos \beta - \delta \sin (A + \beta) (1 - \sin A) \right]$$

For small f , δ and β , this value is always negative and therefore the maximum value of F is assumed to be at a point located between the entering point and the trailing edge on the portion of the surface belonging to the upper side.* On the

* Generally the point is located on the upper side. It lies between the entering point and the leading edge, only when δ is very small in comparison with f . For $\delta = 0$, it lies on the leading edge.

other hand, it can be shown that the maximum is located not far from the entering point. In fact the greatly preponderating member in the numerator of $\tan \psi_0$, on account of formula 8, is $\cos \beta \sin \beta$. The case is not quite so simple with the denominator, which is

$$a^2 + \sin^2 \beta =$$

$$= \frac{4}{l^2} \left[\delta^2 \cos^2 (A + \beta) - \delta f \cos (A + \beta) \sin \beta + \frac{l^2 + f^2}{4} \sin^2 \beta \right].$$

If we introduce into the first member, on the right side of formula 8, the above limit for δ , the denominator is then smaller than $2 \frac{l^2 + f^2}{l^2} \sin^2 \beta$. Hence $\tan \psi_0$ is either smaller or at most only unessentially* greater than $-\frac{1}{2} \cot \beta$, which shows that ψ is either smaller or at most only slightly greater than $\frac{\pi}{2} + 2\beta$. The point ω , at which F assumes its maximum value, is located between the entering point of the streamline and the upper side and, at most, only slightly farther than 4β from the entering point.

Lastly, it may be remarked that in formula 6 for $\frac{1}{F^2}$, both the powers, $\tan^2 \psi$ and $\tan \psi$, appear to be multiplied by small coefficients. Both these members therefore assume quite large values for large values of $\tan \psi$, i. e., in the immediate vicinity of the entering point and the leading edge. Hence F differs but little over the whole surface, with the exception of the specified region, from the value $\cos (A + \beta)$ on the trailing edge and therefore only slightly from unity.

* "Unessentially" means that the deviations are of the order of magnitude f/l , δ/l .

II

The results of the computations in I are as follows: A Joukowski wing is characterized by the three dimensions, namely, the length $2l$, the camber f and the radii difference δ , which is expressed in the thickness of the wing. To these is added the angle of attack β . The points on the surface are most conveniently computed with the aid of a variable ω of the angle at the center of the circle in Fig. 1. The formulas for the coordinates will not be given here. In practice, a graphic process is employed which is explained in the accompanying note by E. Trefftz (pages 130-131 of this same volume of "Zeitschrift für Flugtechnik und Motorluftschiffahrt.") We require only the following data: $\omega = 0$ gives the trailing edge; $\omega = \pi - 2A$ ($\tan A = \frac{f}{l}$) gives the leading edge and the intermediate values of ω correspond to the lower surface of the wing. $\omega = \pi - 2A - 2\beta$ gives the entering point, i.e., the point where the air flow strikes the surface and hence where the velocity is zero.

The ratio of the absolute velocity q of the air flow on the wing to the velocity V in infinity is given by

$$\frac{q}{V} = \frac{\sigma^2}{r} \frac{l}{2} F \quad (5)$$

$r = \frac{\sqrt{l^2 + f^2}}{2} + \delta$ is the radius of the circle in Fig. 1 and

σ the distance OB in the same figure. Both factors, σ and F, depend on ω . For small f and δ , the value of the factor $\frac{\sigma^2}{r \frac{l}{2}}$ differs but little from unity. The properties of the factor F, as obtained by the calculations of I, can be summarized as follows.

On the trailing edge, F has the value $\cos(A + \beta)$ and decreases at the customary angles of attack (about 6°), from the leading edge to the entering point, where it becomes zero. For small f and δ , the decrease takes place very slowly throughout most of the lower side and first becomes rapid in the immediate vicinity of the entering point.

From the entering point, F increases rapidly and attains near the leading edge, a maximum of the order of magnitude $\beta l / 2\delta$. This is approximately also the maximum value of the velocity ratio $q : V$. For this maximum value, the ratio of the angle of attack to the thickness of the wing is therefore decisive, the camber having, in the first order, no effect on it. In constructive wing shapes, where δ and β are of the same order of magnitude, the velocity at the leading edge is accordingly not very great. This result is important because it explains the effect of rounding the leading edge. The result is still more striking when we consider the radius of curvature ρ of the leading edge. It is, namely, with unessential omissions $\frac{\rho}{l} = 16 \frac{\delta^2}{l^2} \left(1 - 4 \frac{\delta}{l}\right)$. The radius of curvature therefore diminishes rapidly with decreasing δ , the rounding

off of the leading edge being very slight, and the maximum velocity remains within moderate bounds. The negative pressure on the leading edge, which, according to Bernouilli's equation, is proportional to q^2/V^2 , is computed by the introduction of the radius of curvature in the first approximation, to $4\beta^2 \frac{l}{\rho}$. I consider this simple formula worthy of attention.

The course of F along the top of the wing can finally be characterized as follows: At some distance from the leading edge, F changes but slowly. If, therefore, the maximum value of F is much greater than unity, it falls abruptly at first and then gradually approaches the value at the trailing edge.

Only in the vicinity of the leading edge does the factor F give us sufficiently accurate information concerning the course of the velocity q . Everywhere else we need to know the course of σ . This can be easily found geometrically from Fig. 1. On the leading edge σ has the value of $l/2$. From the triangle HMO, it follows that σ assumes its minimum value for the angle ω_{\min} , which is given by

$$\frac{\sin \omega_{\min}}{\sin A} = \frac{\frac{l}{2}}{\sqrt{\delta^2 \cos^2 A + r^2 \sin^2 A}}$$

Hence

$$\sin \omega_{\min} = \frac{1}{\sqrt{\frac{4\delta^2}{f^2} + \frac{4r^2}{l^2}}}$$

For the angle $2\omega_{\min}$, we again have $\sigma = \frac{l}{2}$ and then σ

increases further, up to the angle $\omega_{\max} = \omega_{\min} + \pi$. The value of ω_{\min} increases with f/δ . For $\frac{f}{\delta} = 0$, $\omega_{\min} = 0$, hence the value of σ is smallest on the trailing edge and greatest on the leading edge. Conversely, for $\frac{\delta}{f} = 0$, $\omega_{\min} = (\pi/2) - A$ and is therefore situated in the middle of the lower surface. In general, with increasing f/δ , the minimum value of σ moves from the trailing edge to the middle of the lower surface; the point where $\sigma = \frac{l}{2}$ again from the trailing edge to the leading edge, while the maximum value of σ moves simultaneously from the leading edge to the middle of the upper surface.

In order to get an idea of the course of the velocity, we must now estimate the mutual effect of the factors F and σ^2 . I will proceed with this discussion in close connection with the diagrams, which I must first explain. Their arrangement is the same as for the diagrams in Eiffel's "Resistance de l'air." Each figure has, at the bottom, an accurate outline of the wing section. Vertically above each point of the wing, there is plotted from a zero line on the vertical the ratio q^2/V^2 , the upper curve corresponding to the upper side and the lower curve to the lower side of the wing section. The dashed line shows the unit distance from the zero line. The area enclosed by the q^2/V^2 curve gives, when multiplied by $\frac{\gamma}{2g} V^2$, the lift of a unit width of the wing. The chosen angle of attack is 6° ($\beta = 0.1$), the air flow being horizontal.

I am dividing the discussion into several paragraphs.

1. The strong suction on the greater portion of the upper surface is common to all the figures. This is indeed the chief source of the lift, while the pressure on the lower surface contributes only a small increment. This can be easily verified from the general laws. In fact, as already stated, F diminishes very slowly along the under surface from the trailing edge almost to the entering point. Hence, F differs but little, on most of the lower surface, from the value $\cos(A + \beta)$, which it has on the trailing edge, and therefore only a little from unity. Since also the factor $\frac{\sigma^2}{r \frac{l}{2}}$ falls only slightly below 1, up to the vicinity of the entering point, q/V is certainly not much smaller than one and hence there is only a slight pressure.

2. Fig. 2 ($f = 0$ and $\frac{\delta}{l} = \frac{1}{10}$) indeed shows a suction effect along a portion of the under side. Since the values of f are here less than unity, such a suction effect can only be very small. Its appearance is due to relatively large values of σ^2 and depends essentially on the ratio $f : \delta$. Between the trailing edge and $\omega = 2\omega_{\min}$ no suction can occur, because σ is here smaller than $l/2$. Any suction effect can therefore be expected for only small values of $f : \delta$, where ω_{\min} is small. For $\delta = 0$ any suction effect is entirely impossible, since $2\omega_{\min}$ then corresponds to the leading edge.

The suction effect has also been experimentally determined by Eiffel on the wing "en aile d'oiseau" which probably alone of all the surfaces tested by him can be compared with a Joukowski wing section.*

3. Even on the upper side, the course of the velocity is characteristically affected by the ratio $f : \delta$. This is clearly shown by Figs. 2-4. f/δ is expressed on the upper surface in the position of the angle $\omega_{\max} = \omega_{\min} + \pi$, for which σ has its maximum value. The fact that σ continues to increase from the leading edge as far as ω_{\max} causes the maximum value of q to move farther from the leading edge than the maximum of F and the fall in velocity to be less rapid. We differentiate "slightly cambered" wings ($f/\delta < 2$), in which ω_{\max} is near the leading edge, and "highly cambered" wings ($f/\delta > 3$), in which ω_{\max} lies nearer the middle of the upper surface. Fig. 2, with $f = 0$, is a typical example of a slightly cambered wing. Here the maximum value of σ is situated in the leading edge and the values of F and σ therefore decrease

* Eiffel, "Resistance de l'air," 1911, Table XII; also p. 105 and "Complement," p. 192 ("aile Nieuport"). The Eiffel figures show that the suction effect increases on the under side with decreasing angle of attack. This is in agreement with our theory, for the factor F increases, as shown by formula 6, at every point on the under side with decreasing β . Another suction effect, which Eiffel finds on the trailing edge of nearly all wings, is doubtless due to the formation of vortices.

simultaneously, thus producing a very pronounced maximum velocity, although the maximum velocity is not important in itself. On the other hand, Fig. 4 ($f/l = 1/5$, $\delta/l = 1/20$) shows, in spite of a twice as large maximum velocity, a remarkably slow velocity decrease toward the upper side. In fact, in these experiments, the maximum of σ is situated at about $1/3$ of the upper side and a more rapid velocity decrease accordingly first begins behind this point. We note also the small intermediate maximum on the upper side, which is caused by the increase of σ^2 in spite of the simultaneous decrease in F . The mean between Fig. 2 and Fig. 4 is held by Fig. 3, with $f/l = 1/10$ and $\delta/l = 1/20$. Here ω_{\max} does not lie very far from the leading edge, about $1/6$ of the upper side, the increase in σ^2 vanishes under the decrease in F and along the greater portion of the upper side we note a uniform falling off in velocity, due to the simultaneous decrease in the factors F and σ^2 .

These relations were also found in Eiffel's experiments with the wing "en aile d'oiseau." Even the intermediate maximum of q on highly cambered wings is found on his figures.*

Lastly, I wish to call attention to the fact that the measurements of Fig. 4 appear to me to be worthy of commendation, on account of the very uniform stressing of the upper side.

* On Eiffel's figures, it appears that, with decreasing β , the maximum velocity moves backward from the leading edge on the upper side. This also agrees with the theoretical conclusions.

4. Fig. 5 has a very slight rounding ($\delta/l = 1/50$) at $f/l = 1/5$. Therefore $\frac{l}{2} \frac{g}{\delta} = 2.5$ and hence the very high velocity maximum on the leading edge. We have already seen that the high maxima must decrease very rapidly toward the upper side. The region of this steep decline corresponds to an angle of about the size β . During the drop, however, there is in the figure a long space of almost constant velocity. This is explained, as in paragraph 3, by the fact that the maximum value of σ is located at about $1/2.5$ of the upper side. Only behind this point is there again a rapid decline to the trailing edge. This behavior is generally characteristic for highly cambered wings of slight rounding and occurs also on Eiffel's diagrams.

As regards the production of the diagrams, it may be noted, in conclusion, that they were drawn according to the very convenient method of E. Trefftz, as set forth in the accompanying note. Wherever it appeared necessary, the plotting was verified by calculation.

GRAPHIC CONSTRUCTION OF JOUKOWSKI WINGS.*

By E. Trefftz.

In plotting the cross-sectional outline (or profile) of a Joukowski wing, we proceed as follows (Fig. 6).

We first plot an xy system of coordinates with the origin O such that the x axis forms the angle β with the horizontal direction of the wing and mark on the x axis the point L , for which $x = -l$, and on the y axis the point F , for which $y = f$.

We now describe two circles and label them K_1 and K_2 . The center M_1 of the first circle is situated on the straight line LF at a distance 2δ from the point F (beyond the section LF). The circle, moreover, passes through the point L . The second circle likewise passes through the point L and its center M_2 is likewise on LF , the position of M on LF being determined by the following condition. If OV_1 is the portion of the positive x axis cut off by the circle K_1 and OV_2 the portion cut off by the circle K_2 , then

$$OV_1 \times OV_2 = l^2.$$

We now draw, from the point O , the two lines OA_1 and OA_2 , so as to form equal angles with the x axis, A_1 being the point of intersection of the first line with the circle K_1 and A_2 the intersection of the second line with the circle

* From "Zeitschrift für Flugtechnik und Motorluftschiffahrt," May 31, 1913, pp. 130 and 131.

K_2 . Then the center P of the line $A_1 A_2$ is the point sought on the Joukowski wing profile.

In plotting the preceding figures, 24 points were found in this manner for each one, by shifting the first line from the point L 15° each time and drawing the second line symmetrically with reference to the x axis.

In order to determine the pressure on each point of the profile, when the wing is exposed to a horizontal wind having the velocity V , we must know the velocity q at which the air flows by each point of the profile. The pressure on each unit area of the wing surface is then proportional to q^2 .

We can now find the values of q in a very simple manner. For this purpose, we draw a horizontal line through the point L . If we designate by h the distance of the point A_1 (of the circle K_1) from this horizontal line, we obtain, for any desired point P of the figure, the corresponding value of q in the following manner. We take from the diagram the distance between the points A_1 and A_2 , at the middle of which we had found the point P , and also the distances of the point A_1 from the origin O , from the center M_1 of the circle K_1 and from the horizontal line passing through L . We then have

$$q = V \frac{O A_1}{A_1 A_2} \frac{2 h}{M_1 A_1}$$

The mathematical proof for the given constructions is simple. As already mentioned, the profile of a Joukowski wing

can be constructed by describing on the z plane, with the aid of the formula $z = \zeta + \frac{l^2}{4\zeta}$, the circle K , determined by the camber and radii difference. This circle passes through the point $\zeta = -\frac{l}{2}$.

The systems of coordinates are plotted both in the ζ plane and in the z plane in such manner that the ζ axis and the x axis form the angle β with the horizontal wind direction.

If we now describe, in the z plane, both circles, which we obtain from the given circle K in the ζ plane by employing the two conversion formulas

$$z_1 = 2\zeta \quad \text{and} \quad z_2 = \frac{l^2}{2\zeta}$$

then these are the same two circles we designated above by K_1 and K_2 .

The point A_1 has the coordinate z_1 and the point A_2 has the coordinate z_2 , hence the center of $A_1 A_2$ has the coordinate $z = \frac{1}{2} (z_1 + z_2) = \zeta + \frac{l^2}{4\zeta}$, as desired. P is therefore an actual point on the Joukowski curve.

The following formula holds good for the velocity q at which the air flows by every point on the Joukowski figure.

$$q = \frac{\kappa(\xi, \eta)}{\left| \frac{dz}{d\xi} \right|}$$

From $z = \zeta + \frac{l^2}{4\zeta}$ it follows that

$$\frac{dz}{d\xi} = 1 - \frac{l^2}{4\xi^2} = \frac{1}{2\xi} \left(2\xi - \frac{l^2}{2\xi} \right) = \frac{z_1 - z_2}{z_1}$$

whence we obtain

$$\left| \frac{dz}{d\xi} \right| = \frac{A_1 A_2}{O A_1}$$

since the absolute value of $z_1 - z_2$ equals the distance $A_1 A_2$ and the absolute value of z_1 = the distance OA_1 .

For $\kappa(\xi, \eta)$, we obtain, from formula 2 of the preceding article, $\kappa = \frac{2Vh}{M_1 A_1}$, in which h is the distance of the point A_1 from the horizontal line passing through L . In the expression there given for the numerator, it is equal to h and the denominator is equal to $\frac{1}{2}(M_1 A_1)$, as may be easily verified. We thus obtain

$$q = V \frac{2h}{M_1 A_1} \frac{O A_1}{A_1 A_2}$$

which is just the formula given above for q .

Translation by Dwight M. Miner,
National Advisory Committee
for Aeronautics.

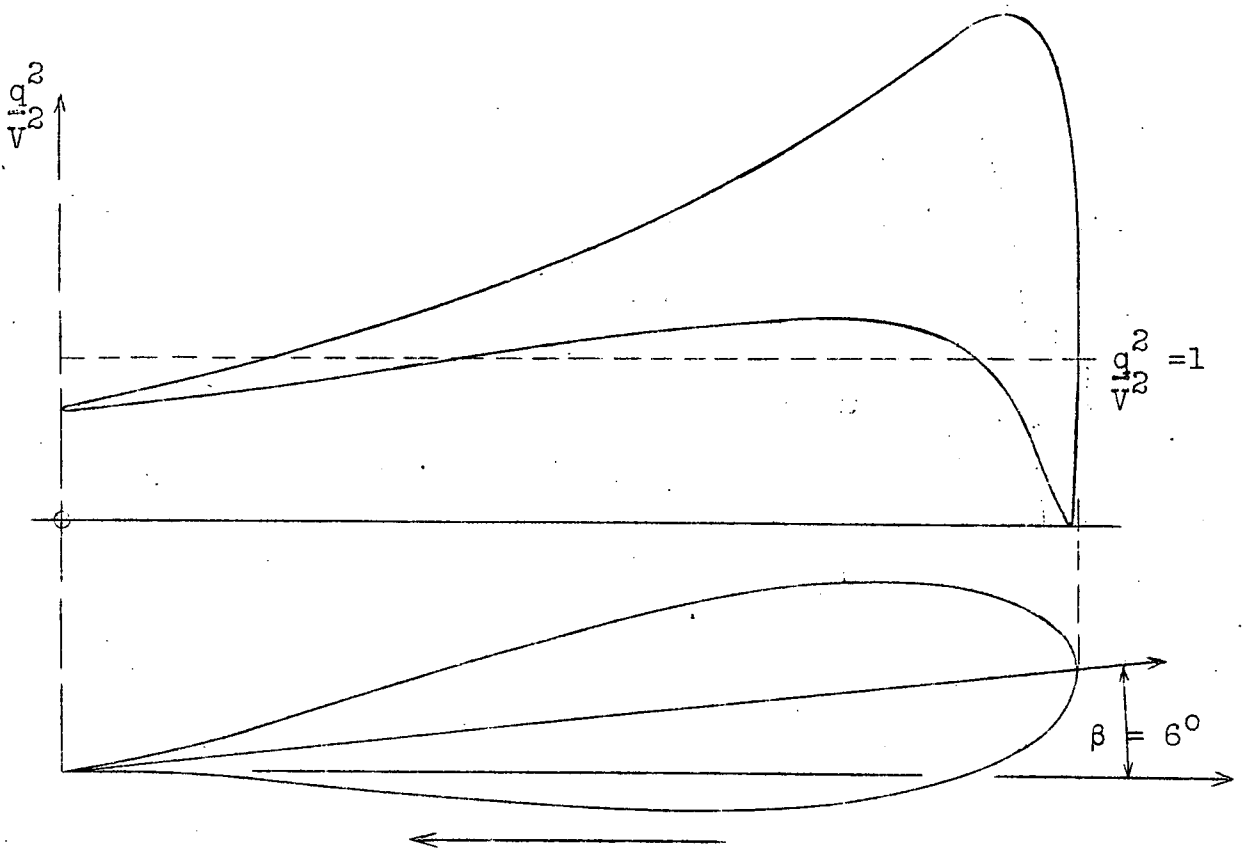


Fig.2: $f = 0,6/z = \frac{1}{10}$

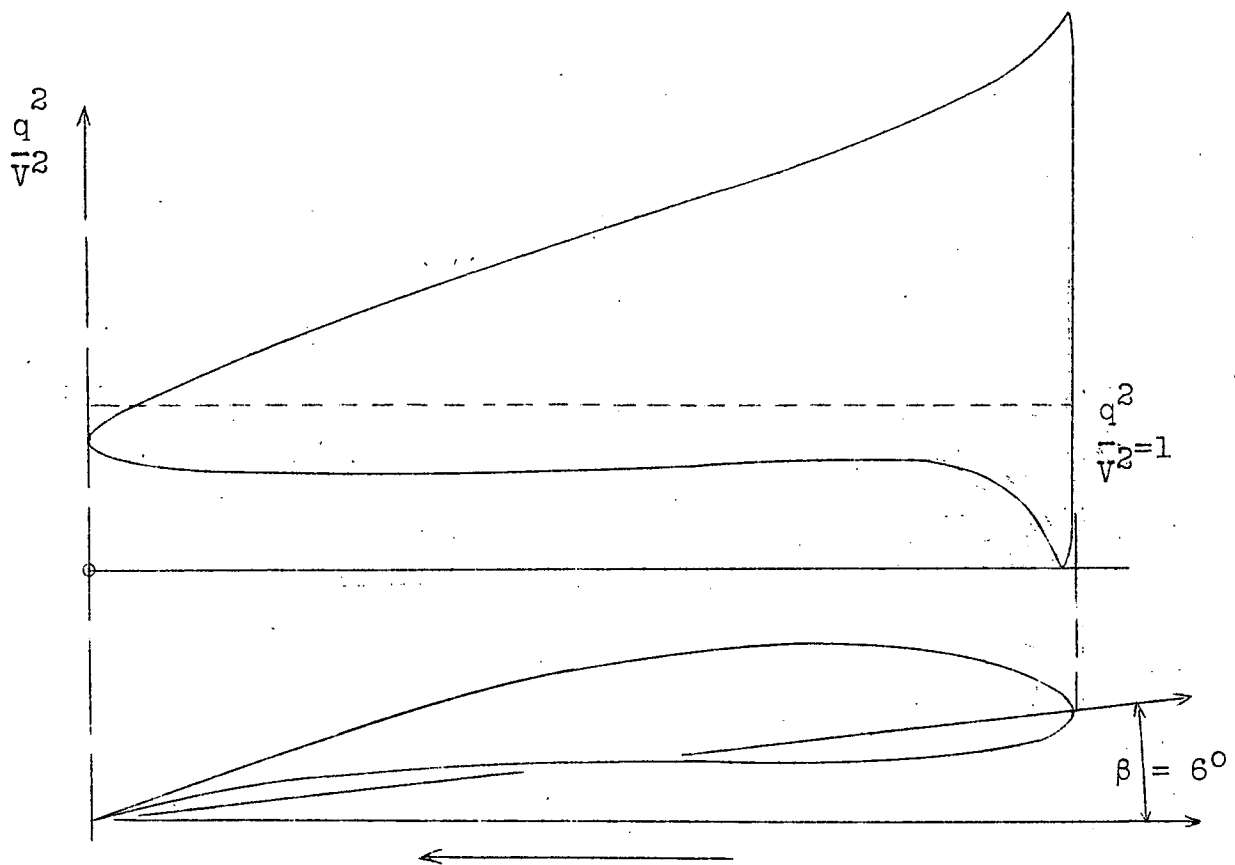


Fig. 3: $f/l = \frac{1}{10}$, $\delta/l = \frac{1}{20}$

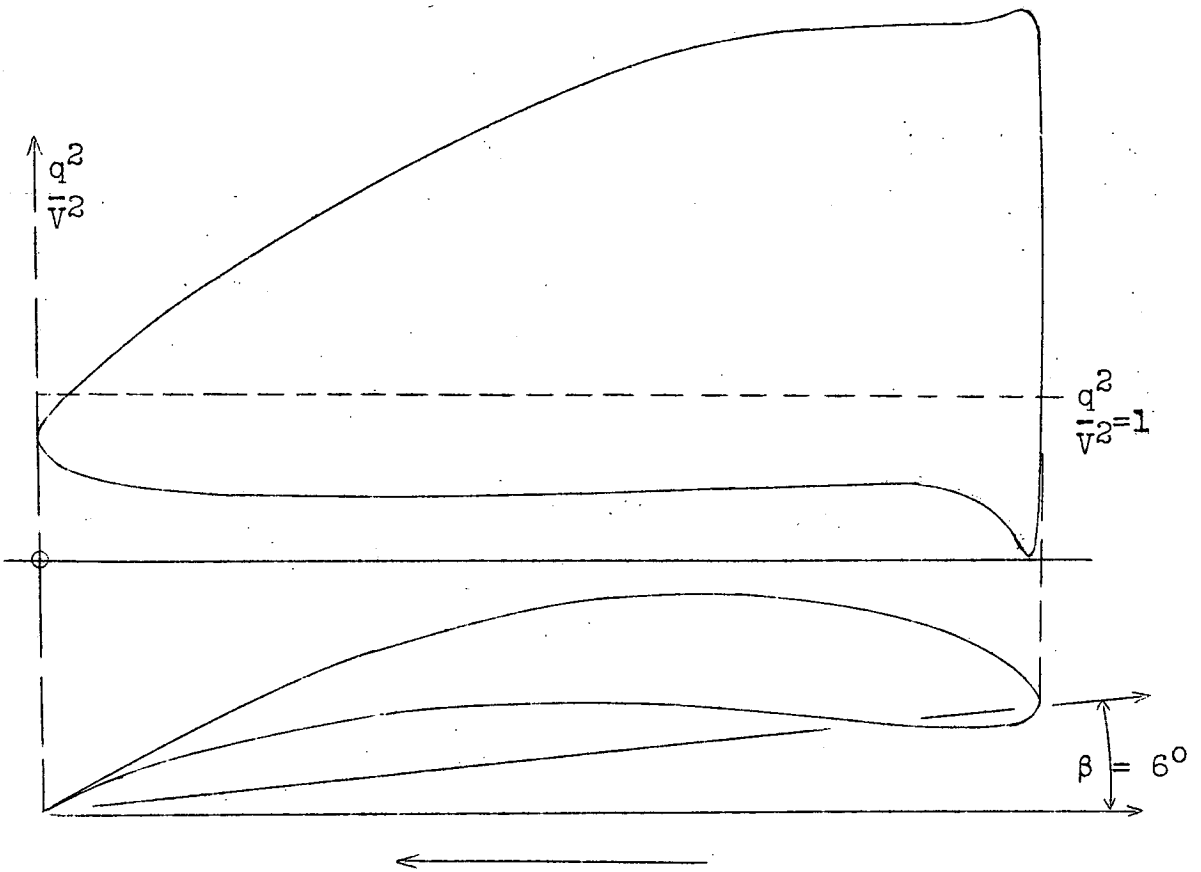
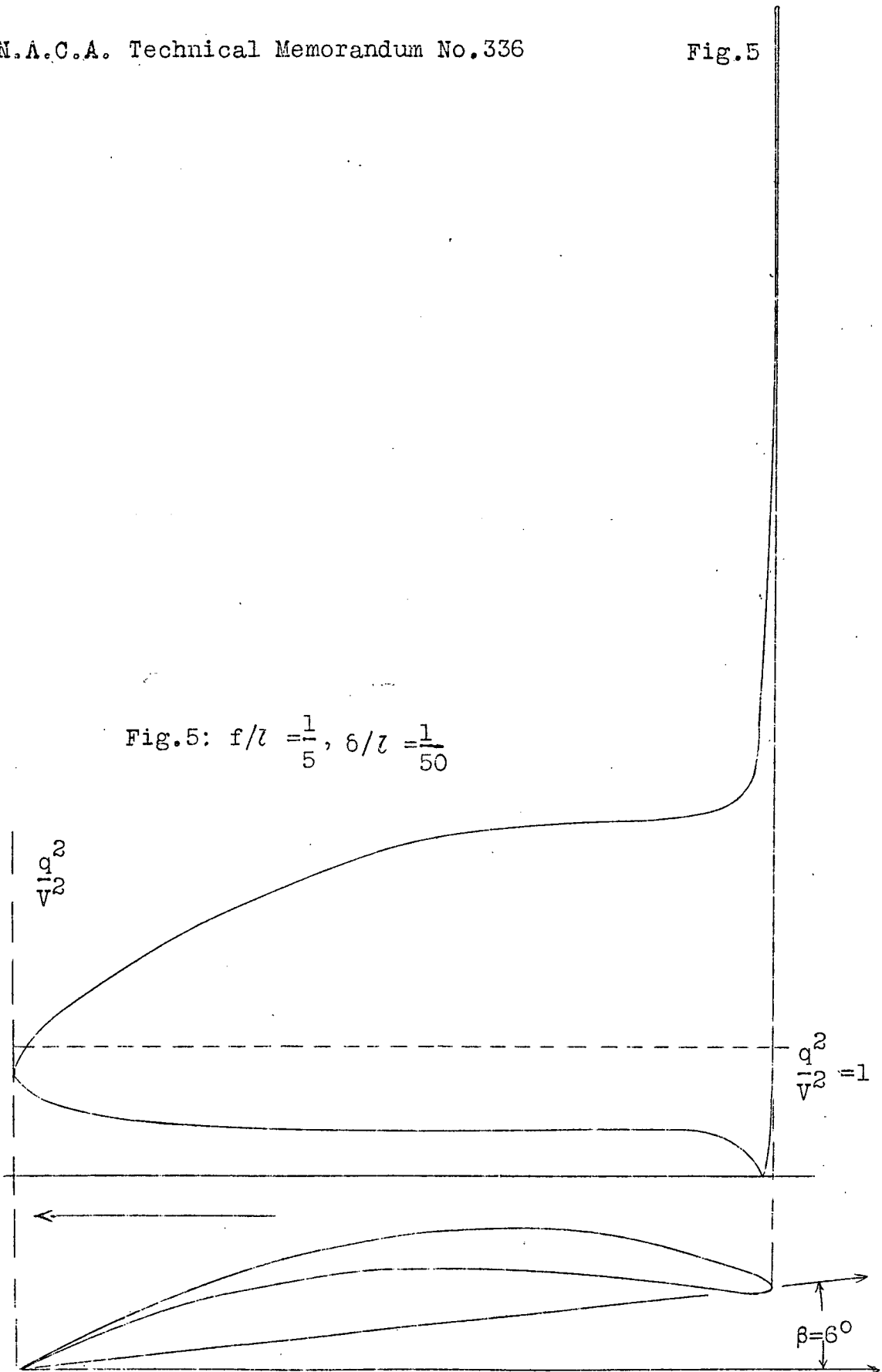


Fig.4: $f/l = \frac{1}{5}$, $\delta/l = \frac{1}{20}$

Fig. 5: $f/l = \frac{1}{5}$, $g/l = \frac{1}{50}$



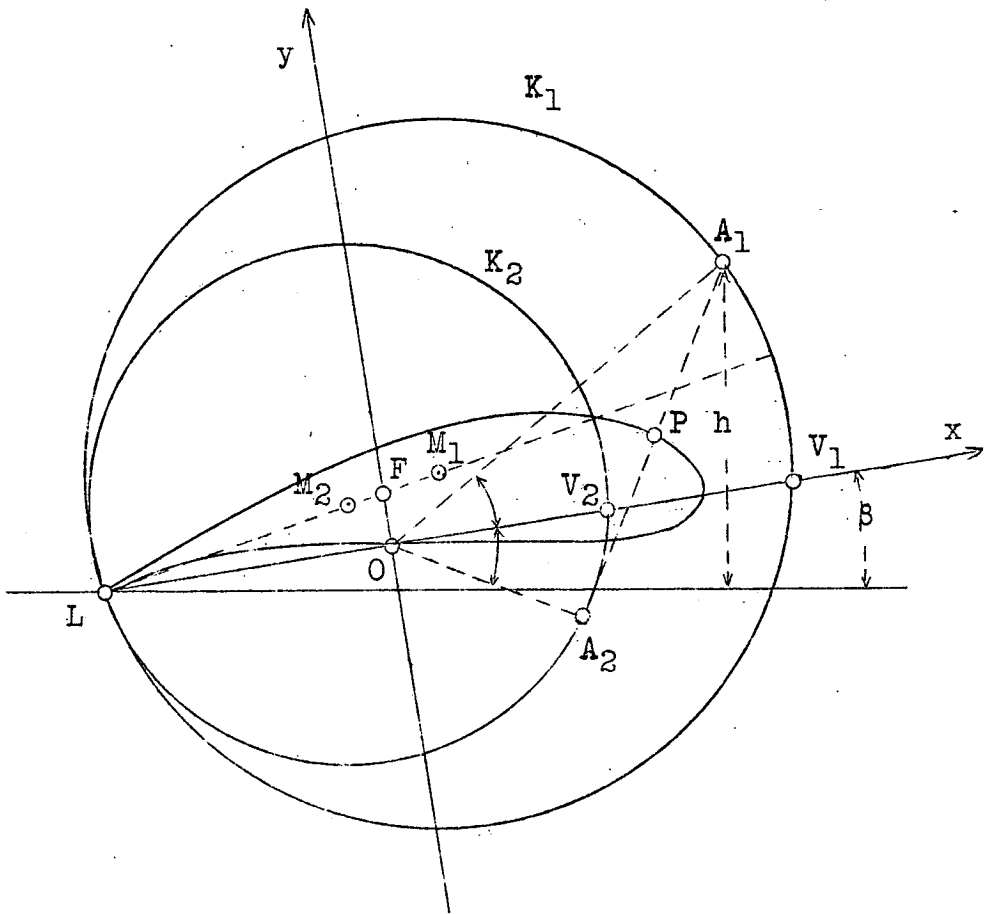


Fig.6